Apodised technique approach for fibre DFB laser design

L. Xia, P. Shum and C. Lu

An apodised technique, applied in fibre distributed feedback laser design, is presented. With the proposed method, the unidirectional output power from the laser is maximised, and the power accumulation in the phase shift region is simultaneously greatly reduced.

Introduction: Fibre distributed feedback (DFB) lasers are attractive devices for a number of applications in the communications and sensing areas [1–6]. Linear cavity lasers based on Bragg gratings written directly in the core of a fibre with different active dopant, such as erbium, ytterbium, neodymium, and thulium, are a promising alternative to semiconductor DBR and DFB lasers. Phase-shifted DFB fibre lasers are attractive owing to their fibre compatibility, compact size, reliability and narrow linewidth. In addition, they have low phase noise as well as low relative intensity noise (RIN).

To suppress the sidelobes and smooth the group delay curve, the apodised technique has been used in grating design for a long time. Recently, the apodised technique has drawn more attention in distributed feedback fibre laser design. Yelen *et al.* have developed a new way of optimising DFB laser cavities [7]. Their method introduced a step-apodised profile that resulted in an increased effective cavity length without changing the reflectivities from their optimum values and without increasing the total grating length. Though the pump-to-signal conversion ratio was increased, a large amount of power accumulation in the phase shift region still existed, which may cause severe Kerr effect and laser instability owing to uneven heating.

A new apodised profile presented in this Letter, which makes the coupling coefficient change smoothly around the phase shift region, can increase the effective laser cavity length and largely reduce the peak power, and unidirectional output power is only slightly affected.

Design method: A numerical analysis of the DFB fibre laser is from the fundamental transfer matrix approach, combined with a model of the erbium-doped fibre. The transfer matrix method, based on the coupled mode solutions for a grating section with constant parameters [8], enables the study of complex fibre laser structures.

We consider now a fibre grating with length $L = 5$ cm and use the Er-doped fibre characters given in [8] and pump with 100 mW at 980 nm. The Bragg period is adjusted according to lasing at 1562 nm. For a variation of local gain $g(z)$ and coupling coefficient $\kappa(z)$, the grating is divided into a number of subsections (typically 100–10 000). The spatial distributions of the forward and backward propagating fields are calculated with the boundary conditions, that there are no in-going signal fields, i.e. $E^{+}(z=0) = E^{-}(z=L) = 0$. In our proposed method, we set the π shift position z_π in the middle of the grating. The coupling coefficient distribution $\kappa(z)$ is determined by

$$\kappa(z) = \begin{cases} \kappa_1 + (\kappa_0 - \kappa_1)/z_\pi * z & (z \le z_\pi) \\ \kappa_0 + (\kappa_2 - \kappa_0)/z_\pi * (z - z_\pi) & (z > z_\pi) \end{cases}$$

where, κ_1, κ_0, κ_2 are the coupling coefficients that exist in the left end, middle, and the right end of the grating, respectively. To make the unidirectional output power (right end output P_1) maximum, κ_1, limited by the photosensitivity of the fibre in practice, is set larger than κ_2, for the reflectivity in the left section of grating should be higher than the right one. Here, κ_1 is chosen to be 350 m^{-1}. First, we select several κ_0 by changing κ_2 from 150 to 300 m^{-1}. The output power P_1 is illustrated in Fig. 1. For a fixed κ_0, the output power P_1 increases with κ_2 at the beginning, and reaches a maximum value, then decreases later. When κ_2 is small, the reflectivity in the right section of the grating is no longer the high reflectivity required in the optimum lasing condition, which induces the output power P_1 lower. However, when κ_2 is as large as κ_1, the power in the laser cavity is divided nearly equally into bidirections, which also makes the unidirectional output power decrease. For example, when κ (=350 m^{-1}) is uniform along the grating length, the output power P_1 is only 3.64 mW. If the step-apodised profile is used ($\kappa_1 = 350$ m^{-1}, $\kappa_2 = 250$ m^{-1}), the calculated value is as arrowed in Fig. 1. Although it is slightly larger than the optimum output power in our apodised profile, the power accumulation is focused mainly around the short π shift zone with the peak power of several hundred watts (see Fig. 4). The optimum value κ_2 can be found to be 250 m^{-1} in Fig. 1. Next, we fix κ_2 (=250 m^{-1}) and compare the results for different κ_0. The κ distributions are shown in Fig. 2. In Fig. 3 we demonstrate the bidirectional output powers, and in Fig. 4, we give the corresponding power distributions. From Fig. 3, it is seen that the output power from the other side P_2 is about one order of magnitude smaller than P_1. With κ_0 increasing, the peak power in the DFB cavity shown in Fig. 4 also increases enormously. Considering the trade-off between the unidirectional output power and the peak power in the DFB cavity, the optimum values can be selected as $\kappa_1 = 350$ m^{-1}, $\kappa_0 = 100$ m^{-1}, $\kappa_2 = 250$ m^{-1}.

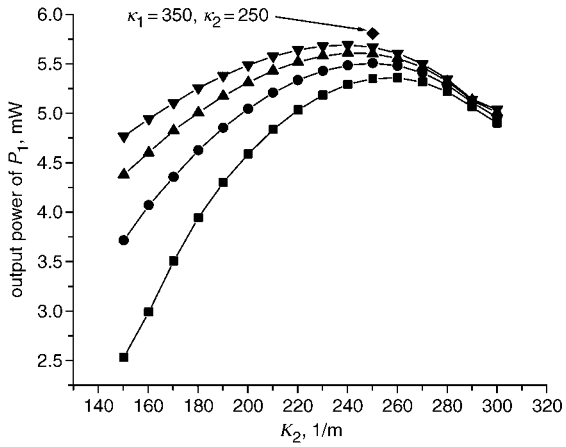

Fig. 1 *Output power against* κ_2

–■– $\kappa_1 = 350$, $\kappa_0 = 0$
–●– $\kappa_1 = 350$, $\kappa_0 = 50$
–▲– $\kappa_1 = 350$, $\kappa_0 = 100$
–▼– $\kappa_1 = 350$, $\kappa_0 = 150$

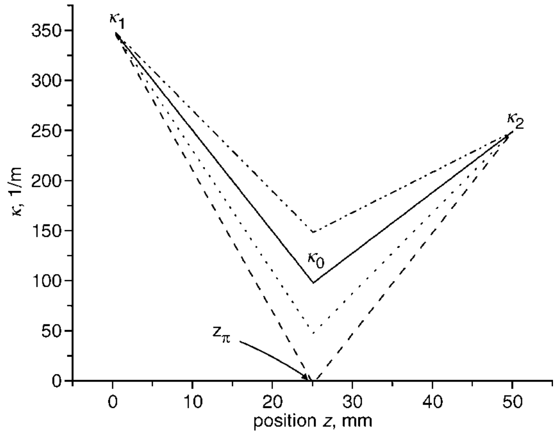

Fig. 2 *Different* κ *distribution*

------------ $\kappa_0 = 0$
.... $\kappa_0 = 50$
———— $\kappa_0 = 100$
–· ·–· · $\kappa_0 = 150$

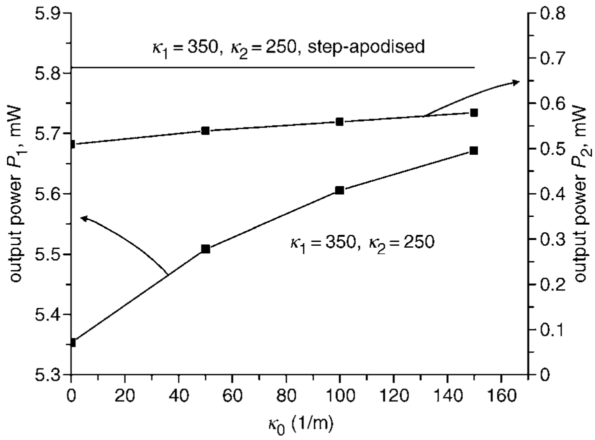

Fig. 3 *Bidirectional output powers*

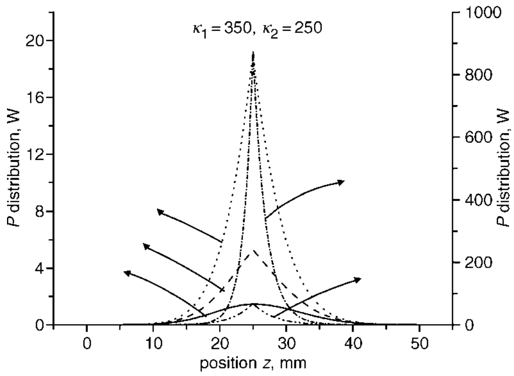

Fig. 4 *P distribution along laser length*

——— $\kappa_0 = 0$
----------- $\kappa_0 = 50$
.... $\kappa_0 = 100$
– · · – · · $\kappa_0 = 150$
– · – · – · step-apodised

Discussion: According to [7], changing the π shift position can make the unidirectional output power maximum. We also calculate the result using the step-apodised profile ($\kappa_1 = 350\ \text{m}^{-1}$, $\kappa_2 = 250\ \text{m}^{-1}$). The π shift position locates in approximately 23.5, 1.5 mm deviation from the middle of the grating, and the output power P_1 is 6.0 mW. The output power P_1 from our optimum apodised profile is only 0.39 mw lower, while the peak power in the laser cavity decreases from nearly 1000 to about 20 W. We believe that the output power drop can be compensated for through setting κ_1 to a higher value, adjusting the reflectivity of the left section to be its optimum value.

Our proposed method can fulfil the requirement of unidirectional output with no need to change the π shift position, which can reduce the π shift introduced complexity. Another advantage is, at the same time, to largely reduce the peak power in the laser cavity, which alleviates the Kerr nonlinearly effect and makes the laser more stable.

Conclusion: An apodised profile is applied in the fibre distributed feedback laser design. With the proposed method, the unidirectional output power from the laser is maximised, and the power accumulation in the phase shift region is simultaneously greatly reduced.

Electronics Letters online no: 20052236
doi: 10.1049/el:20052236

L. Xia, P. Shum and C. Lu (*Network Technology Research Centre, School of Electrical and Electronic Engineering, Nanyang Technological University, Singapore 637553*)

E-mail: xiali@ntu.edu.sg

References

1 Hubner, J., Varming, P., and Kristensen, M.: 'Five wavelength DFB fiber laser source for WDM systems', *Electron. Lett.*, 1997, **33**, (2), pp. 139–140
2 Ibsen, M., Alam, S.U., Zervas, A.N., Grudinin, A.B., and Payne, D.N.: '8- and 16-channel all-fiber DFB laser WDM transmitters with integrated pump redundancy', *IEEE Photonics. Technol. Lett.*, 1999, **11**, pp. 1114–1116
3 Ronnekleiv, E., Ibsen, M., and Cowle, G.J.: 'Polarization characteristics of fiber DFB lasers related to sensing applications', *IEEE J. Quantum Electron.*, 2000, **36**, pp. 656–664
4 Hadeler, O., Ibsen, M., and Zervas, M.N.: 'Distributed-feedback fiber laser sensor for simultaneous strain and temperature measurements operating in the radio-frequency domain', *Appl. Opt.*, 2001, **40**, (19), pp. 3169–3175
5 Løvseth, S.W., and Stepanov, D.Y.: 'Analysis of multiple wavelength DFB fiber lasers', *IEEE J. Quantum Electron.*, 2001, **37**, pp. 770–780
6 Brochu, G., LaRochelle, S., and Slavík, R.: 'Modeling and experimental demonstration of ultracompact multi-wavelength distributed Fabry-Pérot fiber lasers', *J. Lightwave Technol.*, 2005, **23**, pp. 44–53
7 Yelen, K., Hickey, L.M.B., and Zervas, M.N.: 'A new design approach for fiber DFB lasers with improved efficiency', *IEEE J. Quantum Electron.*, 2004, **40**, pp. 711–720
8 Lauridsen, V.C., Søndergaard, T., Varming, P., and Povlsen, J.H.: 'Design of distributed feedback fibre lasers'. ECOC 97, WE1C, pp. 39–42